

Macroscopic evidence of soliton formation in multiterawatt laser plasma interaction

M Borghesi

Department of Pure and Applied Physics, The Queen's University, Belfast

D H Campbell, A Schiavi, O Willi*

The Blackett Laboratory, Imperial College of Science, Technology and Medicine, London

H Ruhl, N Naumova

Max-Born-Institut, Berlin (Germany)

F Pegoraro

Dipartimento di Fisica, Università degli Studi di Pisa (Italy)

S Bulanov

Russian Academy of Science, Moscow (Russia)

A J Mackinnon

Lawrence Livermore National Laboratory, Livermore (CA, USA)

M Galimberti, L A Gizzi

IFAM-CNR, Pisa (Italy)

R J Clarke, S Hawkes

Central Laser Facility, CLRC Rutherford Appleton Laboratory, Chilton, Didcot, Oxon, OX11 0QX, UK

Main contact email address: *m.borghesi@qub.ac.uk*

** present address: Institut für Laser- und Plasmaphysik, Heinrich-Heine-Universität, Düsseldorf (Germany)*

Introduction

Experiments studying the interaction of ultraintense, ultrashort laser pulses with plasmas provide unique laboratory conditions for the study of the collective nonlinear dynamics of a macroscopic system in the relativistic regime. In addition, investigating the structure of the nonlinear coherent modes in the wake of a short laser pulse is of great practical interest as it shows how the laser pulse energy can be transferred to the electromagnetic fields in the plasma and to fast particles. Coherent structures, such as solitons and vortices are fundamental features of this nonlinear interaction. Indeed, analytical and numerical results¹⁻²⁾ have shown that low-frequency, slowly propagating, sub-cycle solitons can be generated in the interaction of ultra short ultraintense laser pulses with underdense plasmas.

A significant fraction of the laser pulse energy can be trapped in these structures in the form of electromagnetic energy oscillating at a frequency smaller than the Langmuir frequency ω_{pe} of the surrounding plasma. The typical size of these solitons is of the order of the collisionless electron skin depth $d_e=c/\omega_{pe}$. The fields inside the solitons consist of synchronously oscillating electric and magnetic fields plus a steady electrostatic field which arises from the charge separation as electrons are pushed outwards by the ponderomotive force of the oscillating fields.

As yet no direct experimental proof of soliton generation in the laser plasma interaction has been obtained. Indeed the experimental detection of such structures poses phenomenal challenges due to their microscopic scale and to their transient nature.

Here we report the experimental observation of bubble-like structures in proton images³⁾ of laser-produced plasmas, which we interpret as the macroscopic remnants of solitons formed during the interaction with the ultra-intense pulse. The observed structures correspond to localized depletion regions in the cross section of a transverse-propagating proton probe beam. We believe that these are the first experimental observations of quasi-neutral cavitated post-solitons. The bubbles appear as the protons are deflected away by the localized electric field at the edges of the cavitated areas. This

interpretation is supported by computational and analytical results.

Experimental arrangement

The experiment was carried out employing the VULCAN Nd:glass laser operating in the Chirped Pulse Amplification mode (CPA). The VULCAN CPA pulse was split in two separate 1 ps, 1 μm , 20 J pulses (CPA₁ and CPA₂) which were focussed onto separate targets in a 10-15 μm FWHM focal spot giving an average intensity of about 10^{19} W/cm². The experimental arrangement is shown schematically in Figure 1. The CPA₁ pulse was used as the main interaction pulse and focused into a preformed plasma. The plasmas were produced by exploding thin plastic foils (0.3 μm thick) with two 1 ns, 0.527 μm laser pulses at a total irradiance of about $5 \cdot 10^{14}$ W/cm². The delay between plasma formation and interaction was typically 1 ns. The CPA₂ pulse was focussed onto a 3 μm Al foil in order to produce a beam of multi-MeV protons, which were used as a transverse particle probe of the interaction region. This is a diagnostic scheme for detection of electric fields in plasmas recently proposed as proton imaging. The delay between the two CPA pulses could be varied optically.

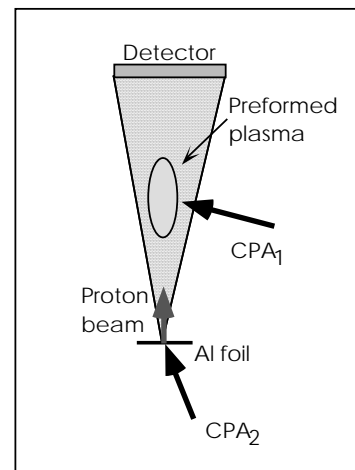


Figure 1. Experimental arrangement.

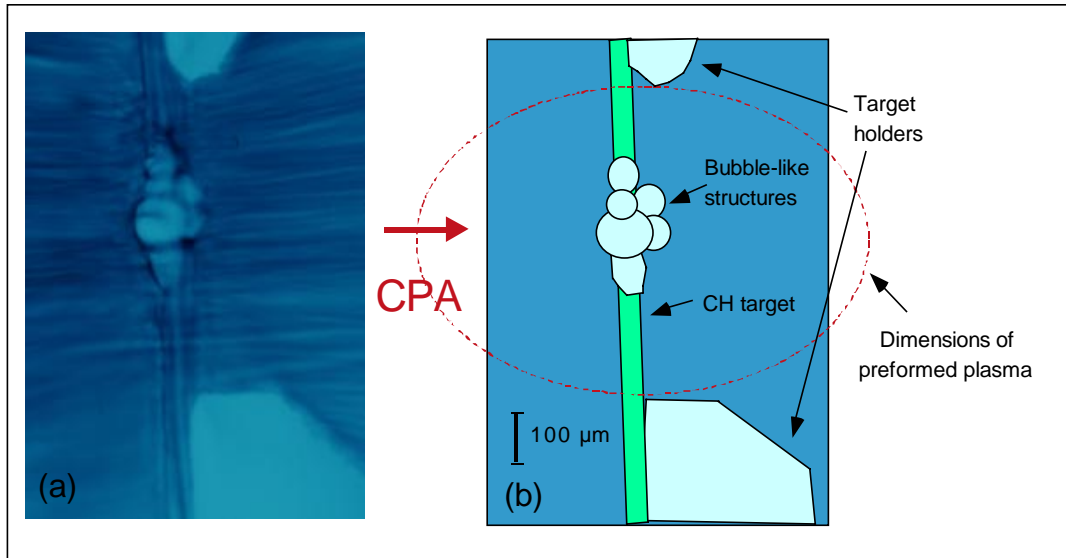


Figure 2. a) Proton image of the preformed plasma taken 20 ps after the CPA₁ interaction with 8 MeV protons. b) Sketch explaining the main features of a).

As the proton source is small, the proton probe could be used in a point-projection imaging arrangement with the magnification determined by the ratio of detector-to-object and object-to-source distances. In our experiment these distances were respectively 2.5 and 22 mm, giving a magnification of about 9.

The proton detector employed consisted of a stack of several layers of radiochromic film (RCF), namely MD-55 GafChromic. The diagnostic use of stacks of RCF for obtaining spectrally selected information on the equivalent dose of the protons stopped is described in Reference 3.

A further, low energy fraction of the CPA pulse was frequency quadrupled and used as a transverse optical probe, alternatively to the particle probe. Interferometry was performed along this line using a modified Nomarsky interferometer, which allowed density characterization of the preformed plasma. The peak density of the plasma was inferred to be 0.1-0.2 n_c @ 1 μm from self-consistent plasma expansion models⁴⁾ and its longitudinal extension was of the order of a mm. By adjusting the delay between the CPA₁ and CPA₂ pulses, it was possible to probe the plasma with the proton beam at different times following the interaction.

Experimental results

The main feature observed in the proton images (i.e. the proton beam intensity cross section after propagation through the plasma) was the onset of several bubble-like structures closely following the interaction. A proton image of the plasma recorded 20 ps after the CPA₁ interaction, and obtained with 8 MeV protons, is shown in Figure 2. Bubble-like structures are clearly visible at the centre of the plasma. In particular, a large structure with radius of approximately 50 μm is seen at the centre of the picture, with five other smaller structures tightly packed around it. The structures are first observed in coincidence with the interaction and appear to survive until about 50 ps after the interaction. At this time the contrast of the bubble structures is much worse than in Figure 2a), and after this time no such structures are clearly observed. The "bubbles" correspond to unexposed regions of the RCF, i.e. regions of the proton beam cross section from which protons have been evacuated. The area density of the matter crossed by the beam is insignificant compared to the stopping range of the protons employed. Therefore it is reasonable to assume that the bubbles are observed in correspondence with plasma regions where localized electric fields, with a component transverse to the proton propagation direction, are present. The region where the bubbles are present extends for about 300 μm in the transverse direction and for about 150 μm in the longitudinal direction.

They are therefore observed even far away from the interaction axis and the vacuum focal spot region. It should be noted that, in similar interaction conditions, break-up of the laser beam in several filaments diverging at wide angles has been observed⁵⁾. This causes fractions of the laser energy to be spread as far as 150 μm (radially) from the propagation axis in the plasma central plane. In presence of this filamentary behaviour, no efficient channel formation process via Coulomb explosion⁶⁾ following the interaction was observed. It is therefore reasonable to assume that the spatial scale of the area occupied by the bubbles in the proton images is consistent with the dimension of the turbulent region left by the laser pulse in the central part of the plasma.

Data interpretation and modelling

We believe that the observations are consistent with structures (post-solitons) deriving by merging of several solitons, and we have supported this assumption with analytical and computational modelling. Detection of solitary structures on time scales longer than the ion motion time brings into play their dynamics under the action of the electrostatic field due to charge separation. As shown in Reference 2, on time scales longer than $\sqrt{m_i/m_e} \omega_{pe}^{-1}$ the nature of the slow propagating subcycle solitons changes because ions start to expand. As a consequence, a void forms in the ion density and the soliton is changed into a radially expanding post-soliton structure that is largely quasineutral. The void in the plasma forms a resonator for the trapped electromagnetic field with frequency ω_s inversely proportional to the post-soliton radius R . As the hole expands, the amplitude and the frequency of the electromagnetic field decrease adiabatically.

From the adiabatic invariant $\int E^2 dV / \omega_s = \text{constant}$ we see that the electromagnetic field amplitude decreases as $E \propto 1/R^2$. Using a snow-plough model of the ion expansion the characteristic expansion time of the post-soliton is found to be given by $\tau = (6\pi R_0^2 n_0 m_i / \langle E_0^2 \rangle)^{0.5}$ with n_0 the plasma density and $R_0 \sim d_e$ and $\langle E_0^2 \rangle / 8\pi$ the initial soliton radius and electromagnetic energy density. For $t/\tau \gg 1$, the post-soliton radius increases as $R \approx R_0 (2t/\tau)^{1/3}$, and the amplitude of the electromagnetic fields and its frequency decrease as $E \sim t^{-2/3}$ and $\omega_s \sim t^{-1/3}$. Their expansion²⁾ makes the post-solitons merge after a certain time, and eventually they form a bubble much larger than the individual solitons. The bubble can even be larger than the volume traced by the laser pulse due to the soliton motion and to the expansion of the plasma as a whole.

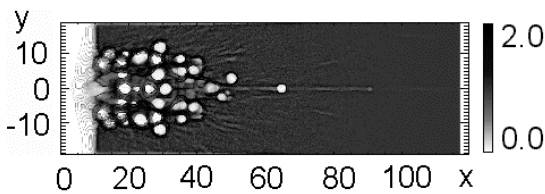


Figure 3. 2-D PIC simulation results: ion density distribution in a cloud of merging post-solitons at $t = 140$.

A laser pulse, wider than a few times d_e , generates a cloud of solitons with conversion efficiency as high as 20% according to the Particle-In-Cell (PIC) results presented in Reference 1. The number N_s of post-solitons depends both on the laser and on the plasma parameters. Figure 3 shows 2-D PIC simulation results, in which a cloud of merging solitons is seen in the wake of a laser pulse. Distances are measured in laser wavelengths λ and times in laser periods $2\pi/\omega$. The laser parameters for these simulations are: dimensionless amplitude $a = 3$, pulse length $l_{||} = 15\lambda$ and width $l_{\perp} = 7.5\lambda$. The laser propagates in an underdense plasma with $n = 0.3n_{cr}$. The figure shows a snapshot of the ion density at $t = 140$. About 30 post-solitons can be seen formed following laser pulse filamentation.

This is a result typically observed in PIC simulations: where the density is not too small compared to the critical density, clouds of solitons are formed, evolve into expanding post-solitons and eventually merge into bigger structures. This process can occur separately at different locations leading to separate macrobubbles. In other words, bubbles appear around each filament if the laser pulse undergoes filamentation inside the plasma. The process of soliton merging is presented in Figure 4, where predictions for an s-polarized pulse with $a = 3$, length $l_{||} = 15\lambda$ and width 7.5λ in a plasma with density $n = 0.3n_{cr}$. The pulse was initialized in such a way as to produce two spatially close solitons, as shown in Figure 4a in the ion density distribution at $t = 80$. As the ions start to move and the two post-solitons expand, their walls intersect going through a transient merging phase that leads to the formation of a new almost circular shell on a time scale of the order of $t = 480$, as shown in Figure 4b.

Similar results appear in the evolution of the ion density pattern shown in Figure 3. At later times than shown in Figure 3, a macrobubble starts to form with a size of the order of the pulse depletion length i.e., of the order of the size of the region inside which the solitons originally formed.

Conclusion

In conclusion the stability, persistence and geometric structure of the "bubbles" observed in the experiment lead naturally to their interpretation in terms of long lived remnants of coherent structures such as solitons, as supported by analytical and PIC modelling. Their "macroscopic" size however is much bigger than the electron skin depth and the time scale over which they are observed implies that the ion dynamics must be accounted for. Post-solitons, and the bubbles formed by their merging, can indeed account for scales much larger than the skin depth and for long expansion times, compatible with the observation time. In addition the values of the electric field that is required in order to account for the proton beam deflection seems to be consistent with the relatively weak electrostatic fields that are expected to occur in the almost quasineutral post-solitons. This field is of the order of the oscillating electromagnetic fields inside the cavity, $E_{||} \approx E_0 a_0 (d_e/R)^4$ and the thickness of the non-quasineutral shell δR is $\delta R/R \sim a_0 (d_e/R)^5$.

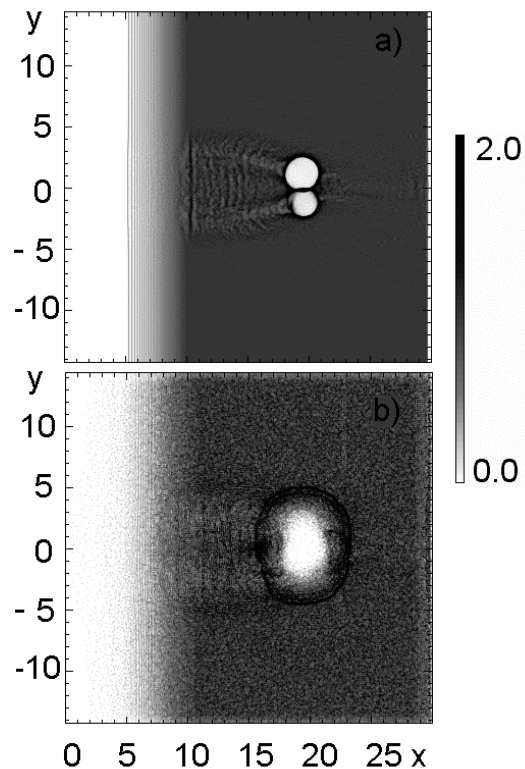


Figure 4. Ion density distributions of two merging post-solitons during (a) and after (b) the merging process, as obtained from 2-D PIC simulations, at $t = 80$ and $t = 480$.

Further modelling is underway in order to support our interpretation, which will include proton tracing through the electric field structures produced by the PIC simulation.

Finally we would like to thank the staff of the CLF for their help and assistance during the experiment.

References

1. S Bulanov *et al*, Phys. Rev. Lett., **82**, 344 (1999);
2. Y Sentoku, *et al*, Phys. Rev. Lett., **83**, 3434 (1999)
3. N Naumova *et al*, submitted to Phys. Rev. Lett. (2001)
4. M Borghesi *et al*, in this Annual report
5. R A London and M D Rosen, Phys. Fluids, **29**, 3813 (1986)
6. M Borghesi *et al*, Proceedings of SPIE, **4424**, 414 (2001);
7. M Galimberti *et al*, Proceedings of SPIE, **4424**, 512 (2001),
8. M Borghesi *et al* Phys. Rev. Lett., **80**, 5137 (1998);